ACS OMEGA

http://pubs.acs.org/journal/acsodf

Article

Photoinduced Antimicrobial Activity of Curcumin-Containing Coatings: Molecular Interaction, Stability and Potential Application in Food Decontamination

Liwei Chen, Ziyue Song, Xiujuan Zhi,* and Bin Du*

Cite This: *ACS Omega* 2020, 5, 31044−31054

Read Online

ACCESS | Metrics & More | Article Recommendations

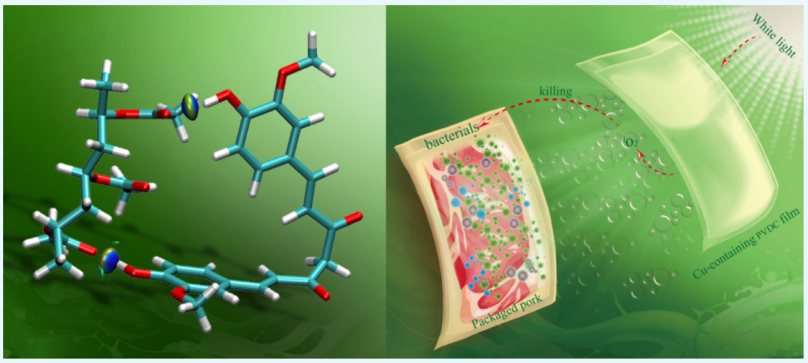

ABSTRACT: Polyvinyl acetate (**PVAc**) and curcumin (**Cu**) were utilized for preparing new protecting **PVAc−Cu$_x$** (x = 1, 5 and 10) coatings exerting antimicrobial photodynamic activity upon white light irradiation. Toward *Salmonella typhimurium* or *Staphylococcus aureus*, the killing efficiency represented the dependence on the **Cu** concentration and irradiation intensity. Toward *S. aureus*, the killing efficiency of **PVAc−Cu$_{10}$** coating reached 93% at an energy density of 72 J/cm^2. With the change in storage time of coating, the results implied significant stability of photosterilization efficiency within 60 days. Compared with the control experiment, lower total viable counts (**TVCs**) and total volatile basic nitrogen (**TVB-N**) values in fresh meat packaged by **PVDC** films with **PVAc−Cu$_{10}$** coatings during storage at 4 °C demonstrated the practicability of the **PVAc−Cu$_x$** coatings in decontaminating fresh pork. **PVAc** packed curcumin tightly within polymer chains, thus preventing tautomerization or, more probably, conformational transition, which is advantageous for improving photostability and emission lifetime.

1. INTRODUCTION

Curcumin (**Cu**), as one of the active components of Indian turmeric, has exhibited potential applications as therapeutic agents against several diseases because of its low toxicity, good anti-inflammatory and antibacterial capabilities, and anticancer activities.[1−5] However, the low solubility and fast degradation assigned to physiological pH and photoinduced instability in aqueous media restrained numerous applications of curcumin in therapeutic agents and photodynamic inactivation (**PDI**) against cancerous cells and pathogenic microorganisms.[6−9] In addition, the equilibrium corresponding to keto- and enol-tautomers, ultrafast excited-state processes closely associated with salvation, and excited-state intramolecular hydrogen atom transfer (**ESIHT**) have been considered important factors affecting its antibacterial and antioxidant capacities in solution.[10−14] Thus, surfactant utilization[15] and encapsulation into delivery systems such as conjugates,[16] nanoparticles,[17−21] molecular complexes,[22] micelles,[23] liposomes,[24] hydrogels,[25] and emulsions[26] have been utilized to improve the solubility, stability, and biocompatibility of curcumin in aqueous media.

After electrons are excited to higher-energy orbitals from the singlet ground state of curcumin (S_0) by means of light illumination, a series of photophysical processes, including the $S_1 \rightarrow S_0$ transition by releasing nonradiative (**NR**) heat energy or radiative fluorescence (**FL**), and $S_1 \rightarrow T_1$ intersystem crossing (**ISC**) will occur. The long lifetime of microseconds of T_1 is usually sufficient for curcumin in the T_1 state to transfer its energy to adjacent normal oxygen ($^3O_2$), generating highly reactive singlet oxygen ($^1O_2$, type **II** reaction), as shown in Figure 1. The toxic singlet oxygen can react with biological

Received: August 22, 2020
Accepted: October 26, 2020
Published: November 20, 2020

https://dx.doi.org/10.1021/acsomega.0c04065
ACS Omega 2020, 5, 31044−31054

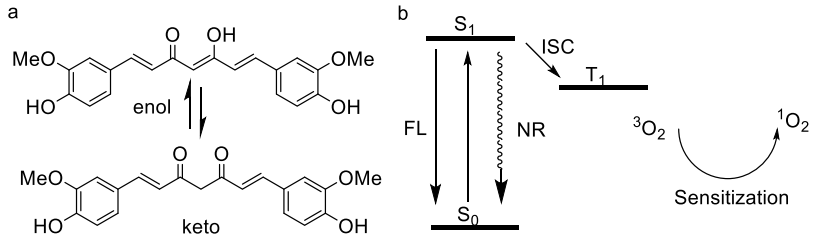

Figure 1. The equilibrium corresponding to keto- and enol-tautomers (a) and the diagram simply describing the energy transfer from $\mathbf{T_1}$ of curcumin to singlet oxygen (b) upon light excitation.

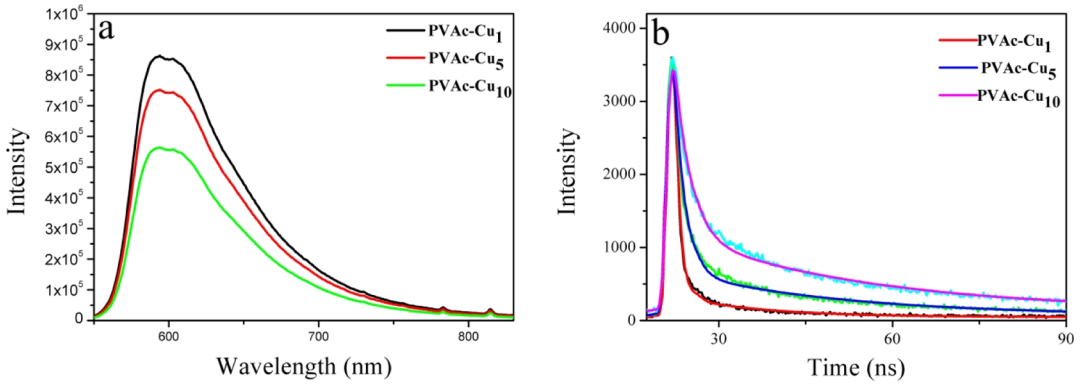

Figure 2. PL emission spectrum (a) and time-resolved lifetime decays (b) of curcumin in **PVAc−Cu$_x$** (x = 1, 5, and 10) coatings. The fluorescence decays of curcumin in emission maxima were measured using the excitation at 442 nm.

molecules such as unsaturated lipids, amino acids of proteins, thus causing cell death and inactivation of microorganisms.[27] The inactivation effect is closely associated with the above-mentioned photophysical processes and the singlet oxygen generation ability of curcumin. The photoinduced inactivation of bacteria based on curcumin was first reported by Tønnesen et al.[28] Haukvik et al. found that curcumin exhibited effective photoinduced antibacterial capacities in aqueous solutions with polyethyleneglycol or Pluronic L35.[29,30] Further, Hegge et al. reported that the phototoxic effect of curcumin with either cyclodextrins or **PEG** 400 in alginate foams proved to be very effective against Gram-positive bacteria.[31]

Recently, active packaging technologies by means of blending chemicals obtained from plants as antioxidant/antimicrobial components into the packaging material have been considered as effective methods to prolong the shelf life of processed food.[32] Owing to its antioxidant/antimicrobial properties, curcumin has been widely used as a food additive in the food processing field and antibacterial films.[33] Pang et al. reported efficient antimicrobial activities of chitosan films containing curcumin-loaded silica nanoparticles for food packaging.[34] Le et al. showed molecular interactions and antimicrobial activity of curcumin−chitosan blend films.[35] Wang et al. fabricated films based on κ-carrageenan incorporated with curcumin for freshness monitoring.[36] However, the antibacterial activities of curcumin as a photosensitizer doped into membranes or coatings are still rarely reported in active food-packaging, and the lack of understanding of the photochemical properties and stability of curcumin in a polymer matrix restrained further development of curcumin in photoinduced antibacterial films for food packaging. The blending of curcumin into a polymer matrix as protecting coatings can offer several advantages over its use as an additive in solution. The rigid microenvironment assigned to a polymer matrix can probably stabilize the curcumin by decreasing ultrafast excited-state processes closely associated with solvation and **ESIHT** under light exposure. In addition, antimicrobial **Cu** coating on the food surface is preferable over the addition of antimicrobials in food formulation owing to higher microbial contamination at the food surface.[37]

Polyvinyl acetate (**PVAc**), with excellent plasticity and strong adhesion, is not soluble with fat and water and utilized as the chewing material of gum sugar and the coating agent of fruit.[38] The biodegradability of **PVAc** with limited hygroscopicity has been proved under certain conditions. It is anticipated that strong interactions may form between the hydroxyl-rich curcumin and the ester linkages abundantly protruding from the polymer backbone. The resulting hydrogen bonds are expected to improve the compatibility between curcumin and **PVAc**, thus inhibiting phase separation and stabilizing curcumin molecules.

The aims of the present work are (i) to present a simple route to efficiently fabricate photoinduced antibacterial **PVAc−Cu** coatings against *Staphylococcus aureus* (Gram-positive) and *Salmonella typhimurium* (Gram-negative) bacteria, (ii) to investigate the photophysical properties of curcumin using steady-state and time-resolved fluorescence spectroscopy for fundamental understanding of excited state and evaluate the stability of photoinduced antibacterial ability with the increase in storage time of coatings, and (iii) to evaluate the practicability of photoinduced antibacterial **PVAc−Cu** coatings deposited on **PVDC** films in decontaminating fresh pork during preservation.

2. RESULTS AND DISCUSSION

2.1. Preparation and Photophysical Properties of the PVAc−Cu$_x$ Coatings. The coating solution containing **PVAc** and curcumin was, respectively, coated on the surface of **PVDC** and **PET** film by utilizing a coating machine. After the wet coat was dried at room temperature for 24 h and vacuum-dried for 6 h to remove ethanol, **PVAc−Cu$_x$** coatings were obtained. The coatings on the surface of stiff **PET** were utilized for the

https://dx.doi.org/10.1021/acsomega.0c04065
ACS Omega 2020, 5, 31044−31054

investigation of photophysical properties, and soft **PVDC** films containing curcumin coatings were utilized to investigate the capability of decontamination of fresh pork. According to the literature, the phototoxicity of photosensitizers toward pathogenic bacteria was closely associated with the dynamic phenomena at excited state, and long-lived excited-state species showed substantial importance in enhanced antibacterial efficiency.[27,39,40] Two fundamental photophysical processes including excited-state hydrogen proton transfer and solvation reorganization will markedly affect the S_1 relaxation of curcumin in solvents, thus leading to short fluorescence lifetimes.[41] However, it is meaningful to investigate the photophysical properties of curcumin in a solid matrix owing to the lack of understanding on the excited state of curcumin in such systems. Fluorescence lifetimes can be fitted with two exponential decays for **PVAc−Cu$_x$** coatings, as shown in Figure 2. As depicted in Table 1, the average fluorescence lifetime at 20 °C was 0.89, 1.29, and 1.95 ns for **PVAc−Cu$_x$** (x = 1, 5, and 10) coatings, respectively. Interestingly, the lifetime increased when the concentration of curcumin content increased in the range of 1−10%, implying the absence of a severe self-quenching effect of the excited state assigned to the aggregation. Severe self-quenching has been proved to reduce the ability for $^1O_2$ generation, thus lowering the efficiency for photoinduced antibacterial ability.[27,39] The comparable curcumin fluorescence lifetimes in water, ethanol, glycerol, and **PVA** films were, respectively, 0.13, 0.12, 0.51, and 0.99 ns, as have been reported by Gryczynski.[10] Sarkar et al. have reported enhanced fluorescence lifetimes of curcumin in nonionic surfactants forming micelles and niosomes, with a maximum of 0.52 ns.[41] This clearly indicated a better stabilization of the excited state of curcumin in the **PVAc** matrix, in comparison with those in solutions or micelles. The polymer film aligned curcumin molecules and packed them tightly within the polymer chains, preventing tautomerization or, more probably, conformational transition. In a hydrophobic **PVAc** matrix, the fast **ESIPT** and solvation process in solutions assigned to short fluorescence lifetimes can probably be inhibited, thus leading to increased lifetime.[10] The change in the lifetime of curcumin in different concentrations also helped us estimate the radiative (k_r) and nonradiative (k_{nr}) rate constants using the published equation. As shown in Table 1, k_{nr} decreased obviously with the increase in the curcumin concentration, implying the change from the duct of deactivation into the radiative decay channels. The corresponding k_{nr} values of curcumin in **PVAc−Cu$_1$** and **PVAc−Cu$_{10}$** were 8.66 × 10^8 and 3.54 × 10^8 s^{-1}, respectively. In comparison with the nonradiative rate constants of curcumin surrounded by silk biomaterials,[8] the values decreased by 1 order of magnitude. When the nonradiative decay of curcumin is reduced, the excited state is saved for fluorescence and **ISC**, which is probably advantageous to singlet oxygen generation.[8,27,39]

Table 1. Fluorescence Lifetime (τ_{av}), Fluorescence Quantum Yields (Φ_f), and Radiative (K_r) and Nonradiative Rate Constants (K_{nr}) of Curcumin in PVAc−Cu$_x$ (x = 1, 5, and 10) Coatings on the Surface of PET Film when Excited at 442 nm

coatings	τ_{av} (ns)	Φ_f (%)	$K_r \times 10^8$ (s^{-1})	$K_{nr} \times 10^8$ (s^{-1})
PVAc−Cu$_1$	0.89	23	2.58	8.66
PVAc−Cu$_5$	1.29	28	2.17	5.58
PVAc−Cu$_{10}$	1.95	31	1.59	3.54

2.2. Molecular Simulation. Molecular simulation was used to investigate the interaction between curcumin and **PVAc** molecules, by modeling the **PVAc** chain as a molecule containing three repeating monomers (**PA3**), as shown in Figure 3. The keto and enol forms coexist in the solid state of curcumin. Toward the keto type, the interaction energy mainly attributed to H-bonding between −OH on the benzene of curcumin and C═O of P**A3** is 26 kcal/mol (structure a), which is larger than the van der Waals interaction between curcumin and **PA3** (16 kcal/mol, structure b). Two hydrogen bonds formed between the hydroxyl of curcumin and the carbonyl group of **PA3** with a distance of 1.78 Å and 1.80 Å, respectively. In addition, the interaction energy mainly assigned to van der Waals between curcumin at the enol type and **PA3** is 22.98 and 16.15 kcal/mol (structures c and d). The results implied that the polymer chains packed curcumin tightly by the occurrence of H-bonding and van der Waals interaction, probably thus leading to the increased stability of curcumin and emission lifetime in solid state.[42]

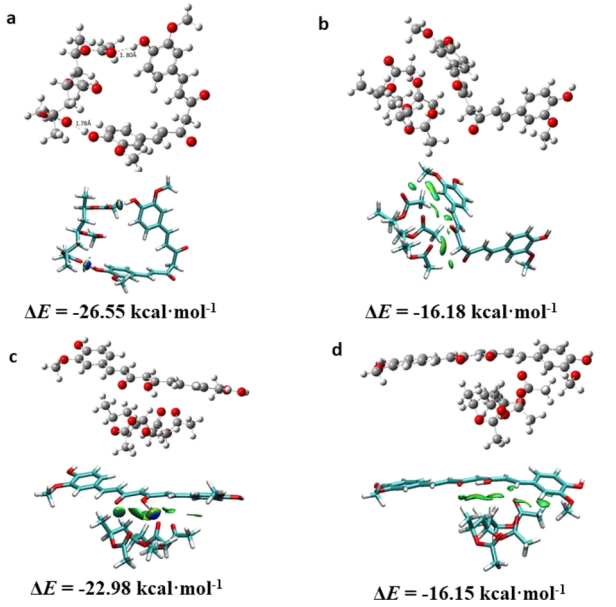

Figure 3. Optimal structures of interaction between **PVAc** molecules and curcumin and surface plots. Structures (a,b) and (c,d) are **PVAc−Cu** interaction at keto and enol types, respectively. H bonds are indicated by a dashed line at structure a.

2.3. Antibacterial Photodynamic Inactivation. Toward *S. aureus*, photodynamic inactivation of bacteria was tested by irradiating coatings at different light fluences. As shown in Figure 4, with the increased concentration of curcumin, the killing efficiency was improved for both the light irradiation and dark cases. In comparison to the dark condition, the killing efficiency obviously increased upon white light irradiation. At an irradiation intensity of 20 mW/cm^2, the killing efficiency is 10, 14, 20, and 28% for **PVAc−Cu$_x$** (x = 0, 1, 5, and 10, respectively) coatings under dark conditions, obviously lower than 15, 42, 55, and 58% under irradiation conditions. Compared with 42% at 20 mW/cm^2, the killing efficiency was increased to 59 and 79%, respectively, for irradiation intensity at 40 and 60 mW/cm^2. Toward *S. aureus*, colony counting showed that the killing efficiency of **PVAc−Cu$_x$** (x = 1, 5, and 10) coatings was 79, 88, and 93% at 60 mW/cm^2 irradiation intensity, respectively, which was obviously higher than values (14, 20, and 28%) in the dark,

https://dx.doi.org/10.1021/acsomega.0c04065
ACS Omega 2020, 5, 31044−31054

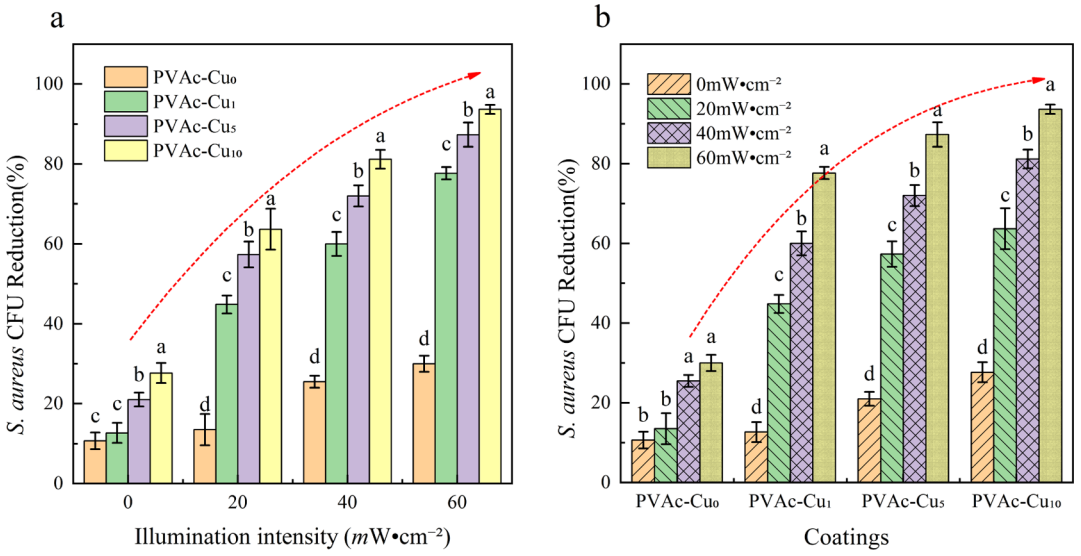

Figure 4. The change trend of biocidal activities (a,b) of **PVAc−Cu$_x$** (x = 0, 1, 5, and 10) coatings against *S. aureus* with increased intensity of irradiation (400−800 nm, irradiation intensity: 20, 40, and 60 mW/cm^2) at an illumination time of 20 min. Different letters marked in the columns show significant difference ($P < 0.05$).

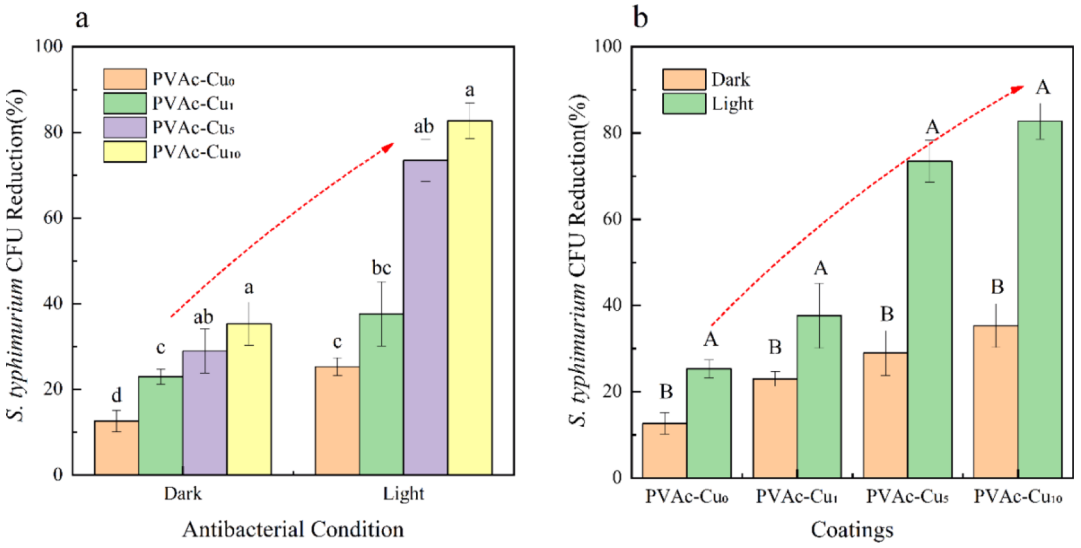

Figure 5. The change trend of biocidal activity (a,b) of **PVAc−Cu$_x$** (x = 1, 5, and 10) coatings toward *S. typhimurium* with the increased concentration of curcumin, under white light irradiation with an intensity of 40 mW/cm^2 at an illumination time of 20 min. Small and capital letters represent significant differences ($P < 0.05$) and highly significant differences ($P < 0.01$), respectively.

indicating the obvious occurrence of photoinduced antibacterial interaction in coatings. The results displayed the synergistic effects of dark and light toxicity from curcumin coatings, and killing efficiency showed the dependence on the concentration and irradiation intensity. With the increase in light intensity, the bacteriostatic properties of the coating increased significantly. Under the same light intensity, an increased curcumin content also improved the bacteriostatic properties of the coatings, and there was a very significant synergistic effect between them ($P < 0.05$).

S. typhimurium can also be efficiently inactivated by light irradiation. Bacterial survival experiments were performed in the dark and white light irradiation, as displayed in Figure 5. With the increase in curcumin concentration, the killing efficiency was gradually improved for both the light and dark cases. Toward *S. typhimurium*, colony counting showed that the killing efficiency of **PVAc−Cu$_x$** (x = 1, 5, and 10) coatings was 38, 73, and 82% at 40 mW/cm^2 irradiation intensity, respectively, which was obviously higher than values in the dark, indicating the occurrence of photoinduced antibacterial properties of coatings. It can be seen that **PVAc−Cu$_x$** coatings have both dark toxicity and phototoxicity and the light intensity and curcumin content in coatings have significant synergy effect on antibacterial capacity.

2.4. Bacterial Morphology and $^1O_2$ Testing. After photodynamic treatment at a radiant exposure of 72 J/cm^2, a clear disruption of the outer membrane of *S. aureus* spores could be observed, probably assigned to $^1O_2$ produced by the curcumin photosensitizer during irradiation. **TEM** was also used to directly visualize the change of *S. typhimurium* bacterial morphology, and flagella disappearance and shape change of the bacteria can be observed in Figure 6d. The generation of $^1O_2$ from **PVAc−Cu$_{10}$** coating under white light irradiation can be detected using the **SOSG** kit. The $^1O_2$ generation of **PVAc−**

https://dx.doi.org/10.1021/acsomega.0c04065
ACS Omega 2020, 5, 31044−31054

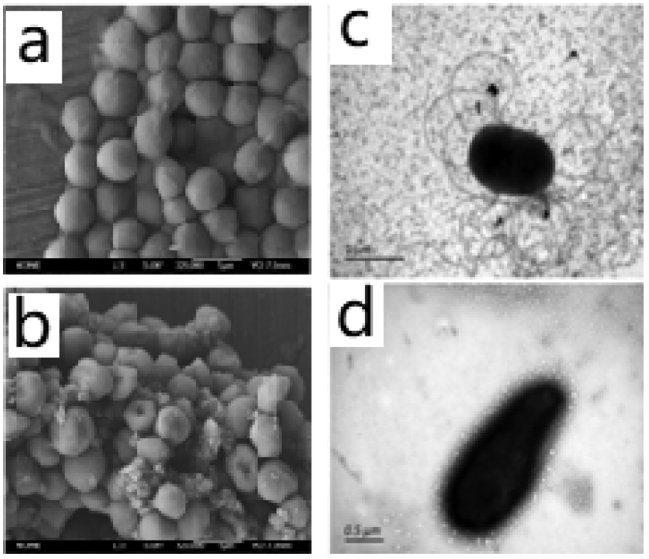

Figure 6. SEM images of *S. aureus* spores (a,b) and **TEM** images of *S. typhimurium* spores (c,d) before and after the photodynamic treatment in the presence of **PVAc−Cu$_{10}$** coating using white light irradiation at a radiant exposure of 72 J/cm^2.

Cu$_{10}$ coating in aqueous solution was measured immediately after light irradiation at 1, 3, and 5 min intervals. It was shown that the total $^1O_2$ generation amount of **PVAc−Cu$_{10}$** at 3 min was appropriately twice as large as that at 1 min, as shown in Figure 7.

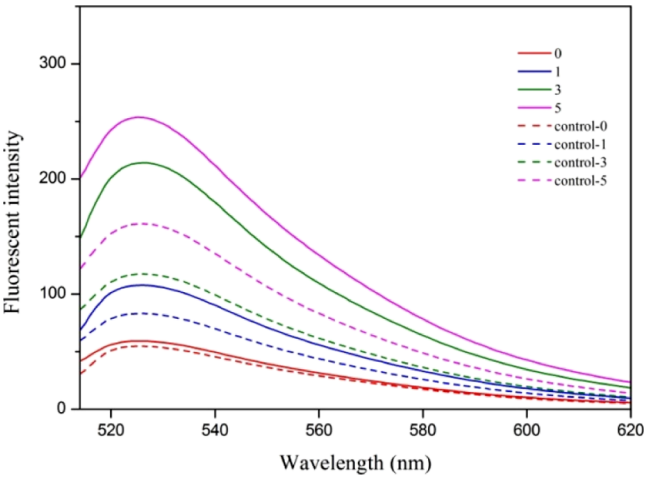

Figure 7. Fluorescence intensity change of **SOSG** as a function of irradiation time (0, 1, 3, and 5 min) at an excitation of 488 nm, in the absence (control samples) and presence of **PVAc−Cu$_{10}$** coating.

2.5. Oxygen Barrier and Microstructure of PVAc−Cu$_x$ Coatings. Soft **PVAc−Cu$_x$** coatings were coated on PET film. The oxygen transmission rates for neat **PET** film at 0% **RH** condition showed ~66.29, 85.47, and 122.21 cm^3/m^2·day at 23, 30, and 40 °C, respectively. In comparison with neat **PET** film, the oxygen transmission rates for **PVAc−Cu$_0$** decreased and showed ~51.61, 66.79, and 99.85 cm^3/m^2·day at 23, 30, and 40 °C, respectively. The oxygen transmission rates for **PVAc−Cu$_1$** at 0% **RH** condition showed ~50.18 cm^3/m^2·day and decreased with an increase in the curcumin concentration (~46.75 and 43.96 cm^3/m^2·day for **PVAc−Cu$_5$** and **PVAc−Cu$_{10}$**, respectively) at 23 °C, implying the concentration dependence of curcumin in the coatings. The results at 30 and 40 °C represented a similar trend at oxygen transmission rates, as shown in Table 2. The results of factorial design analysis showed

Table 2. Oxygen Transmission Rates (OTR, cm^3/m^2·day) of PET Films Coated by PVAc−Cu$_x$ (x = 1, 5, and 10) at 0% Relative Humidity and Different Temperatures

samples	OTR[a]	OTR[b]	OTR[c]
PET−PVAc−Cu$_0$	51.61 ± 1.34	66.79 ± 2.58	99.85 ± 1.24
PET−PVAc−Cu$_1$	50.18 ± 1.58	66.45 ± 1.75	99.45 ± 2.67
PET−PVAc−Cu$_5$	46.75 ± 2.07	61.54 ± 2.24	92.85 ± 3.27
PET−PVAc−Cu$_{10}$	43.96 ± 1.13	58.23 ± 1.70	89.66 ± 1.26

[a]23 °C. [b]30 °C. [c]40 °C.

that concentration and temperature had a significant effect on the oxygen permeation rate. At the same temperature, the oxygen transmittance of the films decreased significantly (P < 0.05) with the increase in curcumin concentration. At the same concentration, the oxygen transmittance of the films increased significantly with the increase in temperature (P < 0.01), as shown in Figure 8.

With the increased concentration of curcumin, the average roughness of the surface decreased in coatings (**PVAc−Cu$_1$**, 3.34 nm; **PVAc−Cu$_5$**, 2.67 nm; and **PVAc−Cu$_{10}$**, 2.24 nm), as shown in Figure 9. SEM photographs revealed the smoother surface of coatings when the curcumin concentration increased. Figure 9 showed the static water contact angle of **PVAc−Cu$_x$** coatings (**PVAc−Cu$_1$**, 59.44°; **PVAc−Cu$_5$**, 60.70°; and **PVAc−Cu$_{10}$**, 64.54°). As shown in Figure 10, the occurrence of a series of 2θ diffraction angles at the range of 5−50 implied the crystallized structure of curcumin powder. No sharp diffraction peaks were observed in **PVAc−Cu$_0$** coating because of the amorphous character of **PVAc**. **PVAc−Cu$_x$** (x = 1, 5, and 10) coatings showed some weak diffraction peaks of curcumin, indicating that the incorporated curcumin was partially crystalline.

2.6. Stability of Coatings in Photoinduced Antibacterials. As reported by many research studies, curcumin was apt to rapidly dissociating into vanillin, ferulic acid, and feruloyl methane in alkaline or neutral solution, probably owing to the presence of the unstable β-diketone linker, and almost half of curcumin will degrade in 30 min in aqueous buffer (pH 7.4) solution. As far as we knew, there were no reports on antibacterial stability of coatings utilizing curcumin as an antibacterial agent under white light illumination. In order to evaluate the antibacterial stability of curcumin in coating, we studied the bacterial killing efficiency of **PVAc−Cu$_1$** coating in the dark and white light irradiation under different storage times. As shown in Figure 11, the antibacterial efficiency of **PVAc−Cu$_1$** against *S. aureus* under light irradiation was much better than that under dark conditions. The bacteriostatic effect slightly decreased with an increase in the storage time. The bacteriostatic efficiency (58.33%) after 30 days was basically stable in comparison with the initial inhibitory efficiency (60%) at 0 day. After 60 days, the antibacterial efficiency of **PVAc−Cu$_1$** decreased significantly from 60 to 47.67% (P < 0.05). The killing efficiency of **PVAc−Cu$_1$** coating increased from 47.67 to 72.60% after 40 min illumination, implying that the duration of light induced a significant increase in the antibacterial efficiency of **PVAc−Cu$_1$** (P < 0.01). The degradation rate of curcumin in **PVAc−Cu$_1$** coating can be estimated by measuring the UV−vis absorption spectrum in solution after the **PVAc−Cu$_1$** coating

https://dx.doi.org/10.1021/acsomega.0c04065
ACS Omega 2020, 5, 31044−31054

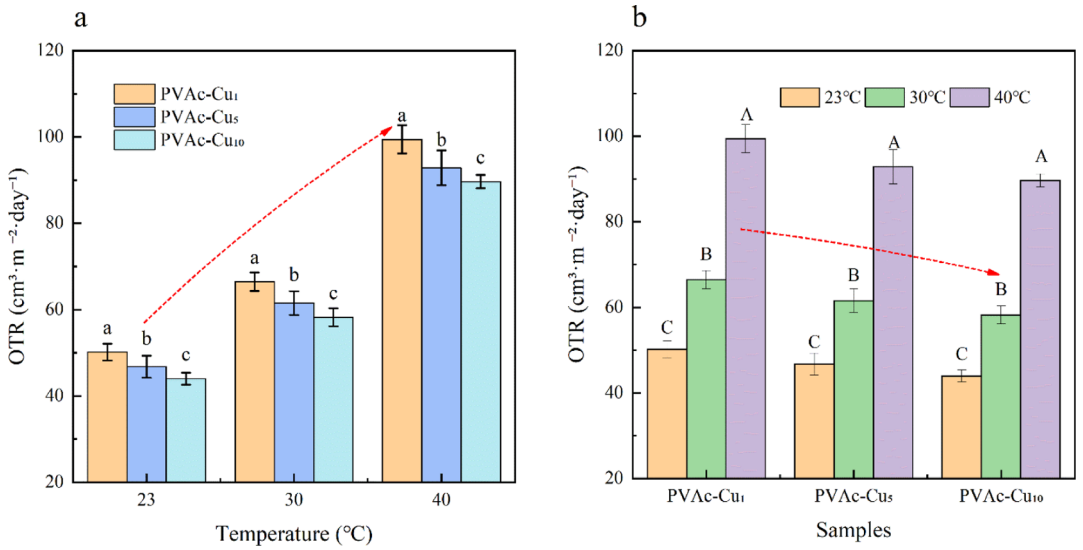

Figure 8. Effect of temperature and concentration (a,b) on oxygen transmission rates of **PVAc−Cu$_x$** (x = 0, 1, 5, and 10) coatings at 0% **RH**. Small and capital letters represent significant differences (P < 0.05) and highly significant differences (P < 0.01), respectively.

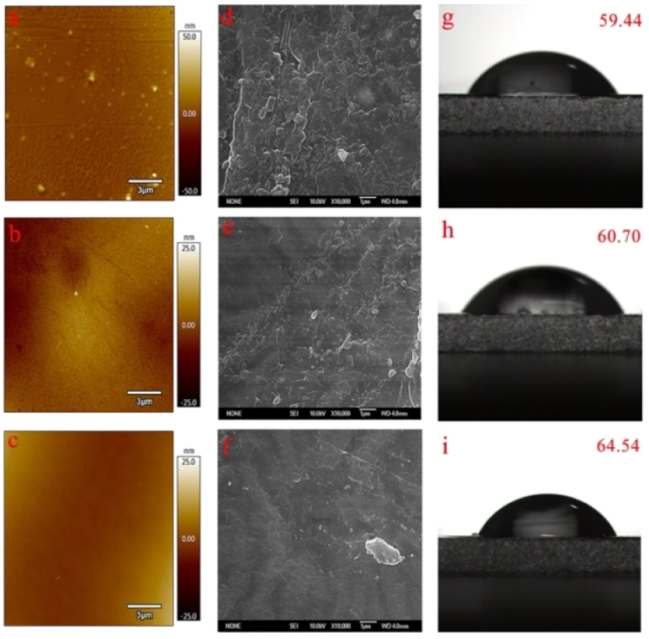

Figure 9. AFM images (a, b, and c for **PVAc−Cu$_1$**, **PVAc−Cu$_5$**, and **PVAc−Cu$_{10}$**, respectively), SEM images (d, e, and f for **PVAc−Cu$_1$**, **PVAc−Cu$_5$**, and **PVAc−Cu$_{10}$**, respectively) and static water contact angles on the surfaces of coatings (g, h, and i for **PVAc−Cu$_1$**, **PVAc−Cu$_5$**, and **PVAc−Cu$_{10}$**, respectively).

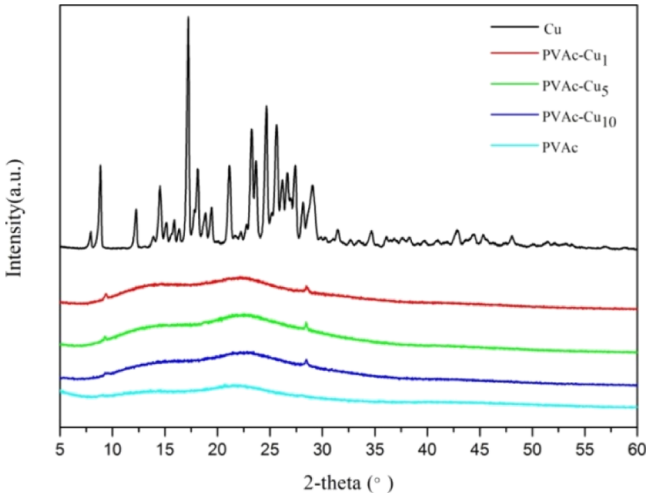

Figure 10. XRD patterns of the curcumin powder and **PVAc−Cu$_x$** (x = 0, 1, 5, and 10) coatings.

was dissolved at different storage time intervals, as shown in Figure 11b. For **PVAc−Cu$_1$** coating stored at room temperature for 60 days, the degradation rate was ∼30% according to the published method[8], while the absorbance peak of curcumin in ethanol rapidly decreased after 14 days, implying that curcumin got better stability in coating than in solution. Our results revealed that the **PVAc** polymeric matrix could act as a good stabilizer for curcumin.

The same coatings were repeatedly used three times to investigate their abilities to retain the antibacterial activity after multiple challenges with *S. aureus* bacteria. The change trend of antibacterial efficiency of **PVAc−Cu$_x$** (x = 1, 5 and 10) coatings against *S. aureus* under white light irradiation at an intensity of 60 mW/cm^2 has been shown in Figure 12. With the increased usage times of coatings, the killing rate decreased, probably assigned to the photodegradation of curcumin after UV sterilization and white light irradiation. However, when the concentration of curcumin was higher than 5%, the antibacterial stability was significantly enhanced. Although the antibacterial rate had a downward trend after repeated usages, there was no significant difference (P < 0.05). The killing efficiency of **PVAc−Cu$_x$** (x = 1, 5, and 10, respectively) coatings was 85.92, 87.92, and 97.93% for the first time, slightly higher than 65.41, 73.03, and 89.60% for the third time. When the irradiation time extended to 30 min at an irradiation intensity of 60 mW/cm^2, the killing rate of **PVAc−Cu$_x$** (x = 5 and 10) can reach 99.9%. However, the long-time light irradiation can result in the photodegradation of curcumin and reduce their capabilities to retain the antibacterial activity after multiple challenges with bacteria.

2.7. Preservation of Fresh Pork Packaged by PVDC Films with PVAc−Cu$_{10}$ Coating under White Light Irradiation. During the storage period, the total viable counts

https://dx.doi.org/10.1021/acsomega.0c04065
ACS Omega 2020, 5, 31044−31054

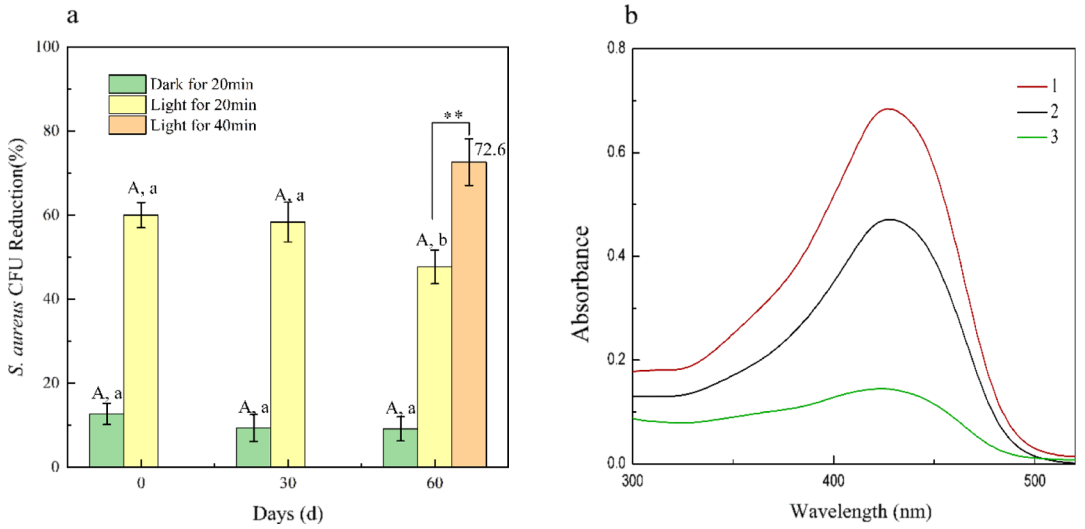

Figure 11. Changes in biocidal activities (a) of **PVAc−Cu$_1$** coating against *S. aureus* under white light irradiation at a light fluence of 48 J/cm^2 (20 min) after storage of 0, 30, and 60 days at 23 °C. The absorption spectrum (b) after **PVAc−Cu$_1$** coating was stored for 0 (1) and 60 (2) days and dissolved in ethanol and the absorption spectrum of curcumin in ethanol after a 14-day interval (3). Small letters ($P < 0.05$) and capital letters and **($P < 0.01$).

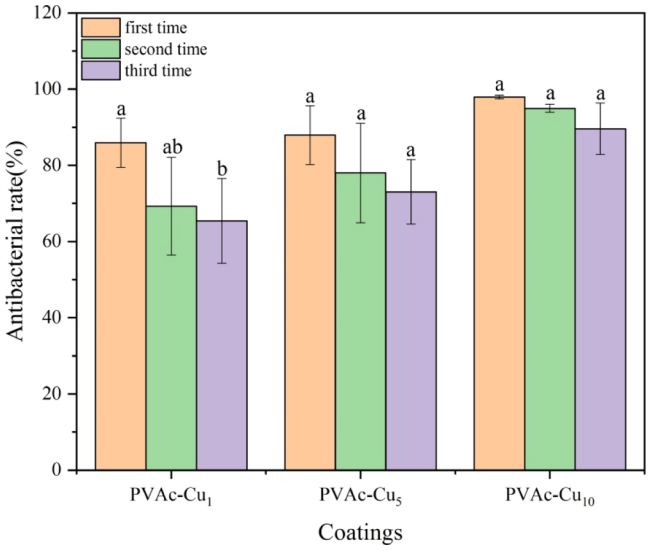

Figure 12. Changes in biocidal activities of **PVAc−Cu$_x$** (x = 1, 5, and 10) coatings against *S. aureus* under white light irradiation at an intensity of 60 mW/cm^2 (20 min) at room temperature, after multiple challenges with bacteria. Small letters ($P < 0.05$).

increased in all groups. The **TVC** value was around 2.2 on the first day, indicating the relatively good quality of pork meat. With the storage time increased, **TVC** values of pork packaged by **PVDC** films with **PVAc−Cu$_{10}$** coating under white light irradiation were lower than those in the control groups and dark conditions, thus proving the occurrence of effective photo-induced antibacterial activities. After 9 days, the **TVC** value at ∼5.4 was still lower than 6.0, which is the critical value of the total bacterial count of meat spoilage. The **TVB-N** value as an indicator to assess meat freshness is closely in association with the meat decomposition caused by bacteria and enzymes during storage. As shown in Figure 13b, the **TVB-N** values of the control groups and dark conditions were obviously higher than those of the irradiated groups with **PVAc−Cu$_{10}$** coating, indicating the effective inhibition of meat degradation attributed to the light irradiation during storage. After the ninth day, the **TVB-N** value at ∼12.5 was still lower than 15.0. However, the **TVB-N** values in other experimental groups exceeded 15.0. According to the previous report, the **TVB-N** value below 15 mg/100 g is the acceptable and appropriate limit for the decontamination of pork meat. The change trend of pH values during storage is shown in Figure 13c. All experimental groups exhibited a clear increasing trend of pH values during cold storage. The pH values of the control groups and dark conditions obviously remained higher than those of the irradiated group with **PVAc−Cu$_{10}$** coating, indicating the effective inhibition of the formation of alkaline substances, such as ammonia, biogenic amines, and trimethylamines, caused by microorganisms and endogenous enzymes.

3. CONCLUSION

In the present work, photoactive **PVAc−Cu$_x$** coatings (x = 1, 5, and 10) were utilized as thin-layer protecting systems for food-packaging purposes. Toward *S. typhimurium* or *S. aureus*, the investigation on biocidal activity of **PVAc−Cu$_x$** coatings demonstrated obvious concentration dependence of curcumin, and the killing effect increased with irradiation time. The killing efficiency of **PVAc−Cu$_{10}$** coating against *S. aureus* reached 93% at 60 mW/cm^2 irradiation intensity in 20 min, indicating the occurrence of effective photoinduced antibacterial interaction in coating. The oxygen transmission rate of coatings will vary with the change in temperature and curcumin concentration. The bacteriostatic efficiency at 58.33% after 30 days was basically stable in comparison with the initial inhibitory efficiency at 60% at 0 day, thus implying the stability of photoinduced antibacterial interaction in coating. The average fluorescence lifetime of **PVAc−Cu$_x$** coatings at 20 °C is 0.89, 1.29, and 1.95 ns. In comparison with fluorescence lifetime of curcumin in solution, the much longer lifetimes in coatings were probably assigned to slower conformational change or tautomerization in a rigid microenvironment, thus leading to stronger stability of curcumin. **TVC** and **TVB-N** values in meat packaged by **PVDC** films with **PVAc−Cu$_{10}$** coatings upon white light irradiation were obviously lower than values in control experiments during storage, demonstrating practicability of the coating in decontaminating fresh pork.

https://dx.doi.org/10.1021/acsomega.0c04065
ACS Omega 2020, 5, 31044−31054

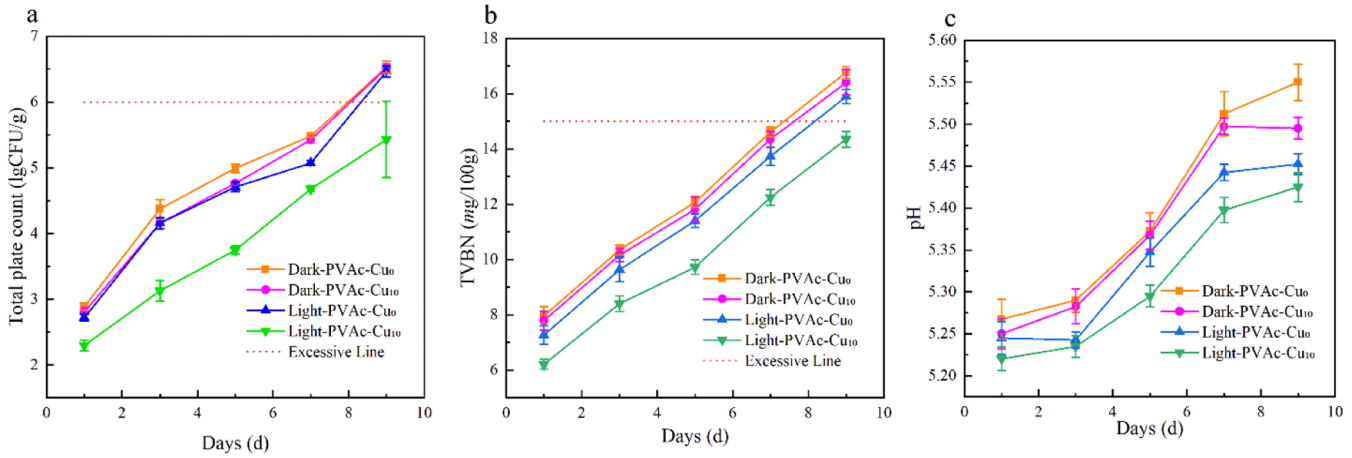

Figure 13. Effect of white light irradiation (15 min, 40 mW/cm^2) on total viable counts [(a) **TVCs**, $\log_{10}$ CFU/g], total volatile basic nitrogen [(b), **TVB-N**, mg/100 g] and pH values (c) of packaged pork by means of **PVDC** films with **PVAc−Cu$_{10}$** coating during storage at 4 °C.

4. MATERIALS AND METHODS

4.1. Materials. Polyvinyl acetate was purchased from Sinopharm Chemical Reagent Co. Ltd. Polyethylene terephthalate (**PET**) and polyvinylidene chloride (**PVDC**) film were obtained from Guanjia Co. Ltd. Curcumin powder with a purity of 98% (J&K Scientific Co. Ltd.) was used without further purification. *S. aureus* and *S. typhimurium* used for the antibacterial experiments were provided by the School of Food Science and Technology in the Beijing University of Agriculture.

4.2. Molecular Simulation. Discrete Fourier transform calculations were performed based on the Gaussian 09 package. The structural optimization was performed at the B3LYP/6-31+g(d) level with Grimme's D3 dispersion corrections. The interaction energy (ΔE) was calculated by the following equation: $\Delta E = E_{\text{Cur−PA3}} - (E_{\text{Cur}} + E_{\text{PA3}})$, where $E_{\text{Cur−PA3}}$, E_{Cur}, and E_{PA3} corresponded to the electronic energy of the curcumin−PA3 complex, curcumin, and PA3, respectively.

4.3. Preparation of the PVAc−Cu$_x$ Coatings. The abbreviation **PVAc−Cu$_x$** (x = 1, 5, and 10%, the weight ratio of curcumin to **PVAc** in coatings) was adopted in the manuscript. The general procedure for the fabrication of **PVAc−Cu$_1$** coating is as follows: the coating solution was prepared by dissolving **PVAc** (2.0 g) powder in ethanol (40 mL) in a magnetic stirrer at 45 °C. Afterward, curcumin (0.02 g) was added to the **PVAc** solution, and the final solution was coated on the surface of **PVDC** and **PET** film by utilizing a coating machine, with a thickness of 0.1 and 1 mm, respectively. After the wet coat was dried at room temperature for 24 h and vacuum-dried for 6 h to remove ethanol, **PVAc−Cu$_1$** coating was obtained. **PVAc−Cu$_5$** and **PVAc−Cu$_{10}$** coatings were obtained by following a similar procedure to prepare **PVAc−Cu$_1$**.

4.4. Equipment and Methods. Contact angles for water drops on coating surfaces were assessed by means of a measurement system (OCA 15EC, Germany) at room temperature. The surface images of the membranes were recorded using an atomic force microscope (Oxford Cypher VRS, UK). Scanning electron microscopy (JEOL Jsm-6700F, JP) was used to visualize the surface of coatings and morphology of *S. aureus*. SEM of *S. aureus*: Bacterial solution irradiated by white light at 60 mW/cm^2 for 20 min at the presence of curcumin coating was centrifuged for 3 min at 4 °C. After removing the supernatant, precipitation was washed with PBS solution three times. Then, glutaraldehyde (2.5%) solution was used to cover the surface of the precipitation and stored overnight at 4 °C after being kept for 6 h at room temperature. After rinsing the sample with PBS solution and centrifuging three times, the bacterial sludge was fixed using the mixed solution of osmic acid and PBS solution at a 1:1 ratio until it blackened. Then, the fixed sludge was washed with PBS three times, and centrifugation removed the supernatant. After gradient dehydration using ethanol (30%, 50%, 70%, 90%, anhydrous ethanol and butanol), the bacterial sludge was placed on a filter paper and frozen at −20 °C for 20 min, followed by freeze-drying in a vacuum freeze dryer for 4 h. The dried bacterial sludge was sprayed with gold for **SEM** observation. At the same time, the control experiment was carried out for comparison. The morphology of *S. typhimurium* was measured using a Hitachi HT-7650 transmission electron microscope (**TEM**). Oxygen transmission rate (**OTR**) values of coatings were obtained using an OX-TRAN model 2/21 instrument at 23 °C and in 0% relative humidity (**RH**). Fluorescence lifetimes were evaluated using a time-correlated single photon counting spectrometer (**TCSPC**, Edinburgh instruments FS5). The average fluorescence lifetimes for the decay curves were calculated from the decay times and the relative contributions of the components using the following equation: $\tau_{\text{av}} = a_1\tau_1 + a_2\tau_2$, where τ_1 and τ_2 are the first and second components of the decay time of curcumin, respectively, and a_1 and a_2 are the corresponding relative amplitudes of these components. Fluorescence quantum yields (Φ_f) were measured in an integrating sphere (IS-080, Labsphere) under the 442 nm line of a HeCd laser.[43] The radiative (K_r, s^{-1}) and nonradiative (K_{nr}, s^{-1}) decay rate constants of curcumin in coatings were evaluated using the following equations: $K_r = \Phi_f/\tau_{\text{av}}$ and $K_{nr} = [1/\tau_{\text{av}}] - K_r$. The generation of $^1O_2$ by coatings upon white light irradiation was determined by the singlet oxygen sensor green reagent (**SOSG**) method.[44] **SOSG** (100 μg) was dissolved in methanol (33 μL) to prepare a solution (5 mM). Then, **PVAc−Cu$_{10}$** coating with 2 × 2 cm^2 was put into plates with a diameter of 35 mm. After deionized water (4 mL) was added, SOSG indicator solution (10 μL) was added, followed by white light irradiation at a light intensity of 60 mW/cm^2 at different time intervals of 0, 1, 3, and 5 min. Finally, the fluorescence spectrum was recorded using a fluorescence spectrophotometer (Varian Cary Eclipse) at an excitation of 488 nm.

https://dx.doi.org/10.1021/acsomega.0c04065
ACS Omega 2020, 5, 31044−31054

4.5. Antibacterial Assessment. Phototoxicity test of coatings toward *S. typhimurium* and *S. aureus* was performed as follows:[45] After both sides of the film were sterilized under ultraviolet light for 15 min, the film was cut into tiny squares of 10×10 mm^2 and placed at the bottom of the well of a 12-well plate with the coated side facing up. A bacterial broth (50 μL, 10^7 CFU/mL) was inoculated onto each test film, and the bacterial broth cultured in the well in the absence of the test film was used as a control. The 12-well plate was protected by transparent plastic cover to avoid the contamination. The wells containing **PVAc−Cu$_x$** coatings and bacteria were incubated in the dark or irradiated by means of an LED lamp (400−800 nm, PLS-LED100, PL-MW 200 photoradiometer, PerfectLight Co. Ltd. China) at a fluence rate of 20, 40, and 60 mW/cm^2 for 20 min, which is corresponding to an energy density of 24, 48, and 72 J/cm^2, respectively. The lamp was placed at a distance of 15 cm above the samples. Then, the coatings with bacteria were washed with **PBS** buffer solution (1 mL, KH_2PO_4/K_2HPO_4, 10 mM, pH 7.4) under ultrasonic treatment for 75 s. After gradient dilution of the phosphate buffer with bacteria, a volume (0.1 mL) of the solution was plated on **LB** agar plates and incubated for 24 h at 37 °C. Viable counts were estimated by a plate count technique. The inhibitory activities (I) under white light irradiation or dark conditions were assessed using the following equation: $I\ (\%) = [(N_1 - N_2)/N_1] \times 100\%$, where N_1 is the total number of bacteria (CFU/mL) in the control sample in the absence of coatings and N_2 is the total number of bacteria of the sample after irradiation or dark conditions in the presence of coatings. The experiment was performed three times.

4.6. Photo-Induced Effect of Curcumin-Containing Coating on TVB-N, TVC and pH Values in the Preservation of Fresh Pork.[46] Fresh meat was purchased from the supermarket and kept at 4 °C in an ice bag. The meat was processed into samples after being preserved in the refrigerator for 1 h. Experimental appliances such as the chopping board, kitchen knife, analytical balance, disposable Petri dish, and aseptic bag were placed on an ultra-clean worktable for ultraviolet sterilization for 30 min. The meat was cut into pieces with a rectangular shape after removing the fat and skin of the meat. The experimental samples were weighed and packaged by **PVDC** films with and without **PVAc−Cu$_{10}$** coating. Both sides of the packaged meat were irradiated for 15 min under white light at an intensity of 40 mW/cm^2. The packaged meat in the absence of irradiation was used as control samples. Finally, all experimental samples were stored in a refrigerator at 4 °C. Total volatile basic nitrogen (**TVB-N**) was estimated by the microtitration method involving steam distillation and titration with HCl. First of all, a sample (20.0 g) was minced and immersed in deionized water (100 mL) for 30 min. The obtained supernatant (10 mL) was mixed with MgO (5 mL, 10 g/L) and was distilled using a Kjeldahl nitrogen apparatus. The distillate was collected with boric acid solution (10 mL, 20 g/L) containing a mixed indicator consisting of methyl red (1 g/L) and methylene (1 g/L) blue in ethanol. Then, the distillation solution was titrated with HCl solution (0.01 M). For comparison, distilled water (10 mL) was used instead of the sample as a blank test. The value of **TVBN** was calculated based on the consumption of HCl using the following equation: $X = \frac{(V_1 - V_2) \times c \times 14}{m \times (10/100)} \times 100$, where V_1 is volume (mL) of HCl used for the sample, V_2 is the volume (mL) of HCl used for the blank, C is the concentration of HCl (mol/L), and m is the weight of the sample (g). Different microorganisms were determined by the spread plate method. The minced sample (25.0 g) was homogenized with 225 mL phosphate buffer solution for 2 min. Further serial decimal dilutions were performed for the determination of microorganisms. A diluting solution (1 mL) was dropped onto the surface of plate count agar and coated evenly, and the plates were incubated at 37 °C for 24 h to calculate total viable counts (**TVCs**). All operations were carried out under aseptic conditions. Plate count agar was selected to determine the total number of spoilage bacteria. The pH values were assessed by inserting a pH meter probe into the fresh meat (Tengtu instrument, testo 205).

4.7. Statistical Analysis. All data were presented as a mean value with their standard deviation (mean ± S.D.). Differences were accepted as significant ($P < 0.05$) and highly significant ($P < 0.01$).

AUTHOR INFORMATION

Corresponding Authors

Xiujuan Zhi − *Beijing Laboratory of Food Quality and Safety, Beijing Key Laboratory of Agricultural Product Detection and Control of Spoilage Organisms and Pesticide Residue, Faculty of Food Science and Engineering, Beijing University of Agriculture, Beijing 102206, China*; Email: 20037504@bua.edu.cn

Bin Du − *Beijing Laboratory of Food Quality and Safety, Beijing Key Laboratory of Agricultural Product Detection and Control of Spoilage Organisms and Pesticide Residue, Faculty of Food Science and Engineering, Beijing University of Agriculture, Beijing 102206, China*; orcid.org/0000-0002-6907-0838; Email: bindu80@bua.edu.cn

Authors

Liwei Chen − *Beijing Laboratory of Food Quality and Safety, Beijing Key Laboratory of Agricultural Product Detection and Control of Spoilage Organisms and Pesticide Residue, Faculty of Food Science and Engineering, Beijing University of Agriculture, Beijing 102206, China*

Ziyue Song − *Beijing Laboratory of Food Quality and Safety, Beijing Key Laboratory of Agricultural Product Detection and Control of Spoilage Organisms and Pesticide Residue, Faculty of Food Science and Engineering, Beijing University of Agriculture, Beijing 102206, China*

Complete contact information is available at: https://pubs.acs.org/10.1021/acsomega.0c04065

Author Contributions

L.C., Z.S. are co-first authors.

Notes

The authors declare no competing financial interest.

ACKNOWLEDGMENTS

This work was supported by grants from the National Science Foundation of China (no. 21772014) and the Scientific Research Program of the Beijing Municipal Education Commission (no. KM202010020003).

REFERENCES

(1) Tsuda, T. Curcumin as a functional food-derived factor: degradation products, metabolites, bioactivity, and future perspectives. *Food Funct.* **2018**, *9*, 705−714.

(2) Chen, R.; Wulff, J. E.; Moffitt, M. G. Microfluidic Processing Approach to Controlling Drug Delivery Properties of Curcumin-

Loaded Block Copolymer Nanoparticles. *Mol. Pharm.* **2018**, *15*, 4517−4528.
(3) Wang, A.; Muhammad, F.; Qi, W.; Wang, N.; Chen, L.; Zhu, G. Acid-Induced Release of Curcumin from Calcium Containing Nanotheranostic Excipient. *ACS Appl. Mater. Interfaces* **2014**, *6*, 14377−14383.
(4) El-Sherbiny, I. M.; Smyth, H. D. C. Controlled Release Pulmonary Administration of Curcumin Using Swellable Biocompatible Microparticles. *Mol. Pharm.* **2012**, *9*, 269−280.
(5) Boztas, A. O.; Karakuzu, O.; Galante, G.; Ugur, Z.; Kocabas, F.; Altuntas, C. Z.; Yazaydin, A. O. Synergistic Interaction of Paclitaxel and Curcumin with Cyclodextrin Polymer Complexation in Human Cancer Cells. *Mol. Pharm.* **2013**, *10*, 2676−2683.
(6) Zhu, J.; Sanidad, K. Z.; Sukamtoh, E.; Zhang, G. Potential roles of chemical degradation in the biological activities of curcumin. *Food Funct.* **2017**, *8*, 907−914.
(7) Bai, F.; Diao, J.; Wang, Y.; Sun, S.; Zhang, H.; Liu, Y.; Wang, Y.; Cao, J. A New Water-Soluble Nanomicelle Formed through Self-Assembly of Pectin−Curcumin Conjugates: Preparation, Characterization, and Anticancer Activity Evaluation. *J. Agric. Food Chem.* **2017**, *65*, 6840−6847.
(8) Panja, S.; Behera, S.; Kundu, S. C.; Halder, M. Optical Spectroscopic and Morphological Characterizations of Curcuminized Silk Biomaterials: A Perspective from Drug Stabilization. *ACS Omega* **2017**, *2*, 6755−6767.
(9) Singh, R.; Tønnesen, H. H.; Kristensen, S.; Berg, K. The influence of Pluronics on dark cytotoxicity, photocytotoxicity, localization and uptake of curcumin in cancer cells: studies of curcumin and curcuminoids XLIX. *Photochem. Photobiol. Sci.* **2013**, *12*, 559−575.
(10) Mukerjee, A.; Sørensen, T. J.; Ranjan, A. P.; Raut, S.; Gryczynski, I.; Vishwanatha, J. K.; Gryczynski, Z. Spectroscopic Properties of Curcumin: Orientation of Transition Moments. *J. Phys. Chem. B* **2010**, *114*, 12679−12684.
(11) Harada, T.; McTernan, H. L.; Pham, D.-T.; Lincoln, S. F.; Kee, T. W. Femtosecond Transient Absorption Spectroscopy of the Medicinal Agent Curcumin in Diamide Linked γ-Cyclodextrin Dimers. *J. Phys. Chem. B* **2015**, *119*, 2425−2433.
(12) Wu, J.; Wang, J.; Zhang, J.; Zheng, Z.; Kaplan, D. L.; Li, G.; Wang, X. Oral Delivery of Curcumin Using Silk Nano- and Microparticles. *ACS Biomater. Sci. Eng.* **2018**, *4*, 3885−3894.
(13) Teng, Z.; Li, Y.; Wang, Q. Insight into Curcumin-Loaded β-Lactoglobulin Nanoparticles: Incorporation, Particle Disintegration, and Releasing Profiles. *J. Agric. Food Chem.* **2014**, *62*, 8837−8847.
(14) Adhikary, R.; Mukherjee, P.; Kee, T. W.; Petrich, J. W. Excited-State Intramolecular Hydrogen Atom Transfer and Solvation Dynamics of the Medicinal Pigment Curcumin. *J. Phys. Chem. B* **2009**, *113*, 5255−5261.
(15) Song, S.; Wang, Z.; Qian, Y.; Zhang, L.; Luo, E. The Release Rate of Curcumin from Calcium Alginate Beads Regulated by Food Emulsifiers. *J. Agric. Food Chem.* **2012**, *60*, 4388−4395.
(16) Safavy, A.; Raisch, K. P.; Mantena, S.; Sanford, L. L.; Sham, S. W.; Krishna, N. R.; Bonner, J. A. Design and Development of Water-Soluble Curcumin Conjugates as Potential Anticancer Agents. *J. Med. Chem.* **2007**, *50*, 6284−6288.
(17) Chen, F.-P.; Ou, S.-Y.; Tang, C.-H. Core−Shell Soy Protein−Soy Polysaccharide Complex (Nano)particles as Carriers for Improved Stability and Sustained Release of Curcumin. *J. Agric. Food Chem.* **2016**, *64*, 5053−5059.
(18) Liu, C.; Cheng, F.; Yang, X. Fabrication of a Soybean Bowman−Birk Inhibitor (BBI) Nanodelivery Carrier to Improve Bioavailability of Curcumin. *J. Agric. Food Chem.* **2017**, *65*, 2426−2434.
(19) Wang, F.; Yang, Y.; Ju, X.; Udenigwe, C. C.; He, R. Polyelectrolyte Complex Nanoparticles from Chitosan and Acylated Rapeseed Cruciferin Protein for Curcumin Delivery. *J. Agric. Food Chem.* **2018**, *66*, 2685−2693.
(20) Sneharani, A. H.; Karakkat, J. V.; Singh, S. A.; Rao, A. G. A. Interaction of Curcumin with β-Lactoglobulin;Stability, Spectroscopic Analysis, and Molecular Modeling of the Complex. *J. Agric. Food Chem.* **2010**, *58*, 11130−11139.
(21) Bhawana; Basniwal, R. K.; Buttar, H. S.; Jain, V. K.; Jain, N. Curcumin Nanoparticles: Preparation, Characterization, and Antimicrobial Study. *J. Agric. Food Chem.* **2011**, *59*, 2056−2061.
(22) Marcolino, V. A.; Zanin, G. M.; Durrant, L. R.; Benassi, M. D. T.; Matioli, G. Interaction of Curcumin and Bixin with β-Cyclodextrin: Complexation Methods, Stability, and Applications in Food. *J. Agric. Food Chem.* **2011**, *59*, 3348−3357.
(23) Banerjee, C.; Ghatak, C.; Mandal, S.; Ghosh, S.; Kuchlyan, J.; Sarkar, N. Curcumin in Reverse Micelle: An Example to Control Excited-State Intramolecular Proton Transfer (ESIPT) in Confined Media. *J. Phys. Chem. B* **2013**, *117*, 6906−6916.
(24) Peng, S.; Zou, L.; Liu, W.; Liu, C.; McClements, D. J. Fabrication and Characterization of Curcumin-Loaded Liposomes Formed from Sunflower Lecithin: Impact of Composition and Environmental Stress. *J. Agric. Food Chem.* **2018**, *66*, 12421−12430.
(25) Harada, T.; Lincoln, S. F.; Kee, T. W. Excited-State dynamics of the medicinal pigment curcumin in a hydrogel. *Phys. Chem. Chem. Phys.* **2016**, *18*, 28125−28133.
(26) Kharat, M.; Du, Z.; Zhang, G.; McClements, D. J. Physical and Chemical Stability of Curcumin in Aqueous Solutions and Emulsions: Impact of pH, Temperature, and Molecular Environment. *J. Agric. Food Chem.* **2017**, *65*, 1525−1532.
(27) Hu, F.; Xu, S. D.; Liu, B. Photosensitizers with Aggregation-Induced Emission: Materials and Biomedical Applications. *Adv. Mater.* **2018**, *30*, 1801350.
(28) Tønnesen, H. H.; de Vries, H.; Karlsen, J.; Beijersbergen van Henegouwen, G. Studies on curcumin and curcuminoids. IX: investigation of the photobiological activity of curcumin using bacterial indicator systems. *J. Pharm. Sci.* **1987**, *76*, 371−373.
(29) Haukvik, T.; Bruzell, E.; Kristensen, S.; Tønnesen, H. H. Photokilling of bacteria by curcumin in different aqueous preparations. Studies on curcumin and curcuminoids XXXVII. *Pharmazie* **2009**, *64*, 666−673.
(30) Haukvik, T.; Bruzell, E.; Kristensen, S.; Tønnesen, H. H. Photokilling of bacteria by curcumin in selected polyethylene glycol 400 (PEG 400) preparations Studies on curcumin and curcuminoids, XLI. *Pharmazie* **2010**, *65*, 600−606.
(31) Hegge, A. B.; Andersen, T.; Melvik, J. E.; Bruzell, E.; Kristensen, S.; Tønnesen, H. H. Formulation and bacterial phototoxicity of curcumin loaded alginate foams for wound treatment applications: studies on curcumin and curcuminoides XLII. *J. Pharm. Sci.* **2011**, *100*, 174−185.
(32) Valdés, A.; Mellinas, A. C.; Ramos, M.; Burgos, N.; Jiménez, A.; Garrigós, M. C. Use of herbs, spices and their bioactive compounds in active food packaging. *RSC Adv.* **2015**, *5*, 40324−40335.
(33) Silva, A. C. d.; Santos, P. D. d. F.; Palazzi, N. C.; Leimann, F. V.; Fuchs, R. H. B.; Bracht, L.; Gonçalves, O. H. Production and characterization of curcumin microcrystals and evaluation of the antimicrobial and sensory aspects in minimally processed Carrots. *Food Funct.* **2017**, *8*, 1851−1858.
(34) Wu, C.; Zhu, Y.; Wu, T.; Wang, L.; Yuan, Y.; Chen, J.; Hu, Y.; Pang, J. Enhanced functional properties of biopolymer film incorporated with curcumin-loaded mesoporous silica nanoparticles for food packaging. *Food Chem.* **2019**, *288*, 139−145.
(35) Liu, Y.; Cai, Y.; Jiang, X.; Wu, J.; Le, X. Molecular interactions, characterization and antimicrobial activity of curcumin−chitosan blend films. *Food Hydrocolloids* **2016**, *52*, 564−572.
(36) Liu, J.; Wang, H.; Wang, P.; Guo, M.; Jiang, S.; Li, X.; Jiang, S. Films based on κ-carrageenan incorporated with curcumin for freshness monitoring. *Food Hydrocolloids* **2018**, *83*, 134−142.
(37) Condat, M.; Mazeran, P.-E.; Malval, J.-P.; Lalevée, J.; Morlet-Savary, F.; Renard, E.; Langlois, V.; Abbad Andalloussi, S.; Versace, D.-L. Photoinduced curcumin derivative-coatings with antibacterial properties. *RSC Adv.* **2015**, *5*, 85214−85224.
(38) Rodriguez, N. L. G.; Thielemans, W.; Dufresne, A. Sisal cellulose whiskers reinforced polyvinyl acetate nanocomposites. *Cellulose* **2006**, *13*, 261−270.

https://dx.doi.org/10.1021/acsomega.0c04065
ACS Omega 2020, 5, 31044−31054

(39) Liu, K.; Liu, Y.; Yao, Y.; Yuan, H.; Wang, S.; Wang, Z.; Zhang, X. Supramolecular Photosensitizers with Enhanced Antibacterial Efficiency. *Angew. Chem., Int. Ed.* **2013**, *52*, 8285−8289.
(40) Li, X.; Lee, D.; Huang, J.-D.; Yoon, J. Phthalocyanine-Assembled Nanodots as Photosensitizers for Highly Efficient Type I Photoreactions in Photodynamic Therapy. *Angew. Chem., Int. Ed.* **2018**, *57*, 9885−9890.
(41) Mandal, S.; Banerjee, C.; Ghosh, S.; Kuchlyan, J.; Sarkar, N. Modulation of the Photophysical Properties of Curcumin in Nonionic Surfactant (Tween-20) Forming Micelles and Niosomes: A Comparative Study of Different Microenvironments. *J. Phys. Chem. B* **2013**, *117*, 6957−6968.
(42) Zhang, Y.; He, H.; Dong, K.; Fan, M.; Zhang, S. A DFT study on lignin dissolution in imidazolium-based ionic liquids. *RSC Adv.* **2017**, *7*, 12670−12681.
(43) Aluigi, A.; Sotgiu, G.; Torreggiani, A.; Guerrini, A.; Orlandi, V. T.; Corticelli, F.; Varchi, G. Methylene Blue Doped Films of Wool Keratin with Antimicrobial Photodynamic Activity. *ACS Appl. Mater. Interfaces* **2015**, *7*, 17416−17424.
(44) Delcanale, P.; Montali, C.; Rodríguez-Amigo, B.; Abbruzzetti, S.; Bruno, S.; Bianchini, P.; Diaspro, A.; Agut, M.; Nonell, S.; Viappiani, C. Zinc-Substituted Myoglobin Is a Naturally Occurring Photoantimicrobial Agent with Potential Applications in Food Decontamination. *J. Agric. Food Chem.* **2016**, *64*, 8633−8639.
(45) Kim, S.; Fujitsuka, M.; Majima, T. Photochemistry of Singlet Oxygen Sensor Green. *J. Phys. Chem. B* **2013**, *117*, 13985−13992.
(46) Sun, X.; Guo, X.; Ji, M.; Wu, J.; Zhu, W.; Wang, J.; Cheng, C.; Chen, L.; Zhang, Q. Preservative effects of fish gelatin coating enriched with CUR/βCD emulsion on grass carp (Ctenopharyngodon idellus) fillets during storage at 4 °C. *Food Chem.* **2019**, *272*, 643−652.

https://dx.doi.org/10.1021/acsomega.0c04065
ACS Omega 2020, 5, 31044−31054